

# QCD and Two-Photon Physics

*Editors: L. Orr, B. Schumm*

## 1 Introduction

A relatively clean environment and well-understood initial state parton content render  $e^+e^-$  colliding beams experiments ideal for both the qualitative confirmation and quantitative testing of Quantum Chromodynamics. Through the years, a number of seminal discoveries and measurements performed at  $e^+e^-$  colliding beam facilities have served to establish the color-charge-based SU(3) gauge theory hypothesis of QCD as the accepted dynamical model of the strong nuclear interaction. Highlights unique to the  $e^+e^-$  QCD program include the discovery of the gluon gauge quantum at PETRA in 1979, the confirmation of the SU(3) gauge structure of quark-gluon and gluon-gluon vertices at LEP in the early 1990's, and the precise measurement of the strong coupling constant  $\alpha_S$  via hadronic observables and  $\tau$  lepton decay.

The study of QCD, and the dynamics of the strong force in general, is expected to provide a significant contribution to the physics program at a high energy  $e^+e^-$  colliding beam facility. The highlights of this program include

- the precise determination of the strong coupling  $\alpha_S$ ;
- the search for anomalous strong couplings of the top quark;
- the study of photon structure; and
- The study of strong-interaction dynamics at high  $\sqrt{s}$  and fixed  $t$ .

Together, these topics constitute a program of study of strong force dynamics which is quite complementary to that of hadron colliders.

## 2 QCD from Annihilation Processes

### 2.1 The Precise Determination of $\alpha_S$

As the single free parameter of the SU(3) gauge theory of the strong interaction, the strong coupling constant  $\alpha_S$  should be measured to the highest available precision. Renormalization-group extrapolations of the U(1), SU(2) and SU(3) coupling strengths act to constrain physics scenarios at the GUT scale; current constraints are limited by few-percent relative precision [1] of the value of  $\alpha_s(M_Z^2)$ . The value of  $\alpha_S$  should also be measured with compatible accuracy over as large a range of scales as possible in order to reveal potential anomalous running in the strength of

the strong interaction. Note that, as a matter of convention, measurements of  $\alpha_s$  performed at other scales are evolved, according to Standard Model renormalization group equations, to the scale  $Q^2 = M_Z^2$ , and quoted in terms of their implied value of  $\alpha_s(M_Z^2)$ .

### 2.1.1 *s-channel Event Observables*

The determination of  $\alpha_s(M_Z^2)$  from the process  $e^+e^- \rightarrow Z/\gamma \rightarrow q\bar{q}(g)$ , using ‘shape’ observables which are sensitive to the underlying parton content, has been pursued for two decades and is generally well understood [2]. In this method one usually forms a differential distribution, makes corrections for detector and hadronization effects, and fits a perturbative QCD prediction to the data, allowing  $\alpha_s(M_Z^2)$  to vary. Examples of such observables are thrust, jet masses and jet rates.

The latest generation of such  $\alpha_s(M_Z^2)$  measurements, from SLC and LEP, has shown that statistical errors below the 1% level can be obtained with samples of a few tens of thousands of hadronic events. With the current Linear Collider design luminosity of  $2.2 \times 10^{34} \text{ cm}^{-2}\text{s}^{-1}$ , at  $\sqrt{s} = 500 \text{ GeV}$ , hundreds of thousands of  $e^+e^- \rightarrow q\bar{q}$  events would be produced each year, and a statistical error on  $\alpha_s(M_Z^2)$  below 0.5% would be achieved.

At energies far above the  $Z^0$  pole, the electron-positron collision cross section is dominated by  $t$ -channel processes such as  $Z^0Z^0$  and  $W^+W^-$  production. In addition, due to the substantial mass of the  $t$  quark, the inclusive characteristics of  $e^+e^- \rightarrow t\bar{t}$  events tend to mimic those of lighter quark events with hard gluon radiation. A prescription for the elimination of these backgrounds developed for the 1996 Snowmass workshop [3,4] makes use of electron beam polarization and precise tracking to reduce the effects of these backgrounds on the measured three-jet rate to less than 5%, with the corresponding systematic uncertainty on the extraction of  $\alpha_s(M_Z^2)$  expected to be substantially less than 1%. In addition, the sizable initial state and beamstrahlung radiation associated with Linear Collider energies will act to smear the cms energy of the  $e^+e^-$  annihilation process, as well as to boost the particle flow into the forward regions of the detector. A PYTHIA study [5], including the full effects of ISR, has shown that these considerations can be accurately taken into account in the measurement of  $\alpha_s(M_Z^2)$ .

Hadronization effects, which lead to corrections of order 10% at the  $Z^0$  pole, are expected to fall at least as fast as  $1/\sqrt{s}$ , leading to corrections of order 1% at  $\sqrt{s} \geq 500 \text{ GeV}$  [6]. The corresponding systematic error on the extraction of  $\alpha_s(M_Z^2)$  is thus expected to be substantially below 1%. Detector systematics, due primarily to limited acceptance and resolution smearing, and which are observable-dependent, are found to contribute at the level of  $\delta\alpha_s(M_Z^2) = \pm 1 - 4\%$  at LEP-II [7]. The greater hermeticity and  $\cos\theta$  coverage anticipated for Linear Collider detectors is again expected to reduce this substantially.

Currently perturbative calculations of event shapes are available complete only up to  $O(\alpha_s^2)$ , although resummed calculations are available for some observables [8]. One must therefore estimate the possible bias inherent in measuring  $\alpha_s(M_Z^2)$  using the truncated QCD series. Though not universally accepted, it is customary to estimate this from the dependence of the fitted  $\alpha_s(M_Z^2)$  value on the QCD renormalization scale, yielding a large and dominant uncertainty of about  $\Delta\alpha_s(M_Z^2) \simeq \pm 6\%$  [2]. Therefore, although a  $\pm 1\%$ -level  $\alpha_s(M_Z^2)$  measurement is possible experimentally, it will not be realized unless  $O(\alpha_s^3)$  contributions are calculated. There is reasonable expectation that this will be achieved within the next 5 years [9].

### 2.1.2 The $t\bar{t}(g)$ System

The dependence of the  $e^+e^- \rightarrow t\bar{t}$  cross section on  $m_t$  and  $\alpha_s(M_Z^2)$  is presented in the chapter on the physics of the top quark. As discussed in that chapter, next-to-next-to-leading order calculations of the  $t\bar{t}$  cross section in the resonance region show that, while the peak of the  $1S$  resonance is stable with respect to cms energy, the normalization of the  $t\bar{t}$  cross section exhibits a substantial renormalization scale dependence. While good news for the extraction of  $m_t$ , this suggests that a simultaneous fit for the strong coupling constant will not yield a systematically precise value of  $\alpha_s(M_Z^2)$ .

### 2.1.3 A High-luminosity Run at the $Z^0$ Resonance

A sample of  $10^9$   $Z^0$  decays offers two additional options for  $\alpha_s(M_Z^2)$  determination via measurements of the inclusive ratios  $\Gamma_Z^{had}/\Gamma_Z^{lept}$  and  $\Gamma_\tau^{had}/\Gamma_\tau^{lept}$ . Both are indirectly proportional to  $\alpha_s$ , and hence require a very large event sample for a precise measurement. For example, the current LEP data sample of 16M  $Z^0$  decays yields an error of  $\pm 2.5\%$  on  $\alpha_s(M_Z^2)$  from  $\Gamma_Z^{had}/\Gamma_Z^{lept}$ , with an experimental systematic of  $\sim \pm 1\%$ . With a Giga- $Z^0$  sample, the statistical error would be pushed to below  $\Delta\alpha_s(M_Z^2) = 0.4\%$ . Even with no improvement in experimental systematics, this would be a precise and reliable measurement. In the case of  $\Gamma_\tau^{had}/\Gamma_\tau^{lept}$  the experimental precision from LEP and CLEO is already at the 1% level on  $\alpha_s(M_Z^2)$ . However, there has been considerable debate about the size of the theoretical uncertainties, with estimates as large as 5% [10]. If this situation is clarified, and the theoretical uncertainty is small,  $\Gamma_\tau^{had}/\Gamma_\tau^{lept}$  may offer a further 1%-level  $\alpha_s(M_Z^2)$  measurement.

## 2.2 $Q^2$ Evolution of $\alpha_s$

In the preceding sections we discussed the expected precision on the measurement of the benchmark parameter  $\alpha_s(M_Z^2)$ . Translation of the measurements of  $\alpha_s(Q^2)$  ( $Q^2 \neq M_Z^2$ ) to  $\alpha_s(M_Z^2)$  requires the assumption that the ‘running’ of the coupling is determined by the QCD  $\beta$ -function. However, since the logarithmic decrease of

$\alpha_S$  with  $Q^2$  is a telling prediction of QCD, reflecting the underlying non-Abelian dynamics, it is essential to explicitly test this  $Q^2$ -dependence. In particular, such a test would be sensitive to new colored degrees of freedom with mass below the limit for pair-production at the highest explored scale. For this measurement of the  $Q^2$  dependence of  $\alpha_S$ , rather than its overall magnitude, many common systematic effects would be expected to cancel. Hence it would be desirable to measure  $\alpha_S$  in the same detector, with the same technique, and by applying the same treatment to the data at a series of different  $Q^2$  scales, so as to maximize the lever-arm for constraining the running.

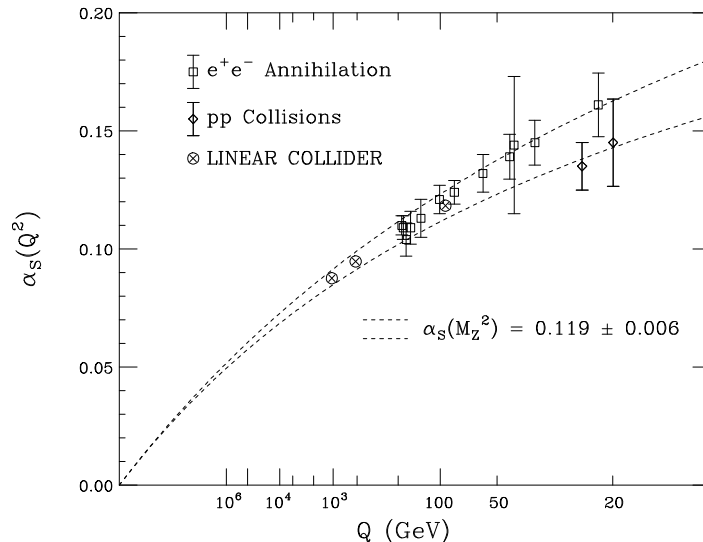


Figure 1: Linear Collider measurements of  $\alpha_s(M_Z^2)$ , in comparison to existing measurements from  $e^+e^-$  and  $p\bar{p}$  collisions, as a function of interaction scale.

Simulated measurements of  $\alpha_s(Q^2)$  at  $\sqrt{s} = 91, 500$  and  $1000$  GeV are shown in Fig. 1, together with existing measurements which span the range  $20 \leq \sqrt{s} \leq 200$  GeV. The Linear Collider point at  $\sqrt{s} = 91$  GeV is based on the  $\Gamma_Z^{had}/\Gamma_Z^{lept}$  technique, while those at  $500$  and  $1000$  GeV are based on event shapes. A theoretical uncertainty of  $\pm 1\%$  is assumed for all LC points.

The Linear Collider data would add significantly to the lever-arm in  $Q^2$ , and would allow a substantially improved extrapolation to the GUT scale. For example, a simultaneous fit for  $\alpha_s(M_Z^2)$  and  $\beta_0$  (the leading term in the expansion of the QCD  $\beta$ -function which establishes the rate at which the strong coupling constant runs; expected to be about  $0.61$  in the SM) leads to a precision of  $\pm 0.0018$  and  $\pm 0.034$ , respectively, for the LC data alone. Including accurate measurements at low  $Q^2$  (particularly from  $e$  and  $\mu$  DIS), the existing constraints are  $\pm 0.0030$  and  $\pm 0.042$ , respectively. Combining existing data with that available from the LC would

yield constraints of  $\pm 0.0009$  and  $\pm 0.016$ , providing a substantial improvement on the measurement of the running of  $\alpha_s(M_Z^2)$ , as well as the extrapolation to the GUT scale (see Fig. 2). Note that, unlike the determination of  $\beta_0$ , the accuracy of the GUT-scale extrapolation is not dependent upon future running at the  $Z^0$ .

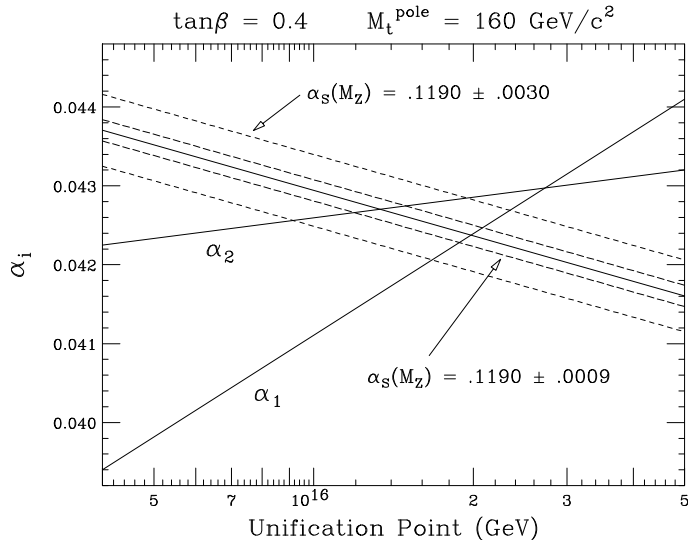


Figure 2: Improvement in the GUT scale constraint, assuming a  $\pm 1\%$  measurement of  $\alpha_s(M_Z^2)$  at the Linear Collider. RG trajectories assume the MSSM with  $\tan\beta = 0.4$  and  $m_t^{\text{pole}} = 160 \text{ GeV}/c^2$  [11].

### 2.3 Top Quark Strong Moments

The very large mass of the recently discovered top quark suggests the possibility that top plays a central role in physics beyond the Standard Model. If this is the case, it is likely that this new physics will manifest itself via anomalous top-quark moments, which represent the low-energy manifestation of effective higher-dimensional couplings.

In the case of the strong interactions of top, the lowest-dimensional gauge-invariant and CP-conserving extension to SM top quark couplings is the anomalous chromomagnetic moment, which we can parameterize via a dimensionless quantity  $\kappa$ . The corresponding chromoelectric moment, parameterized by  $\tilde{\kappa}$ , violates CP and arises from an operator of the same dimension. The resulting generalized three-point  $t\bar{t}g$  vertex takes the form

$$L = g_s \bar{t} T_a (\gamma_\mu + \frac{i}{2m_t} \sigma_{\mu\nu} (\kappa - i\tilde{\kappa}\gamma_5) q^\nu) t G_a^\mu, \quad (1)$$

here  $g_s$  is the SU(3) gauge coupling parameter,  $m_t$  is the top quark mass,  $T_a$  are the SU(3) color generators,  $G_a^\mu$  are the vector gluon fields, and  $q$  is the outgoing gluon four-momentum.

This interaction leads to a substantially different spectrum of gluon radiation for  $e^+e^- \rightarrow t\bar{t}$  events above threshold than for the pure vector interaction case corresponding to  $\kappa = \tilde{\kappa} = 0$ . Fits to this spectrum thus provide limits on the values of  $\kappa$  and  $\tilde{\kappa}$ . Fig. 3, from Ref. [12], shows the limits in the  $\kappa$ - $\tilde{\kappa}$  plane that can be achieved with an integrated luminosity of 100 and 200  $fb^{-1}$  at  $\sqrt{s} = 1$  TeV. Similar studies for the Tevatron and LHC [14] indicate that the corresponding sensitivities at hadron colliders will be substantially weaker, in particular for the case of  $\kappa$ , for which sensitivities of  $|\kappa| < 0.1$  will be difficult to achieve. In [13], the authors offer a technicolor model for which the unique capability of the LC to precisely measure strong moments of top would be a critical asset.

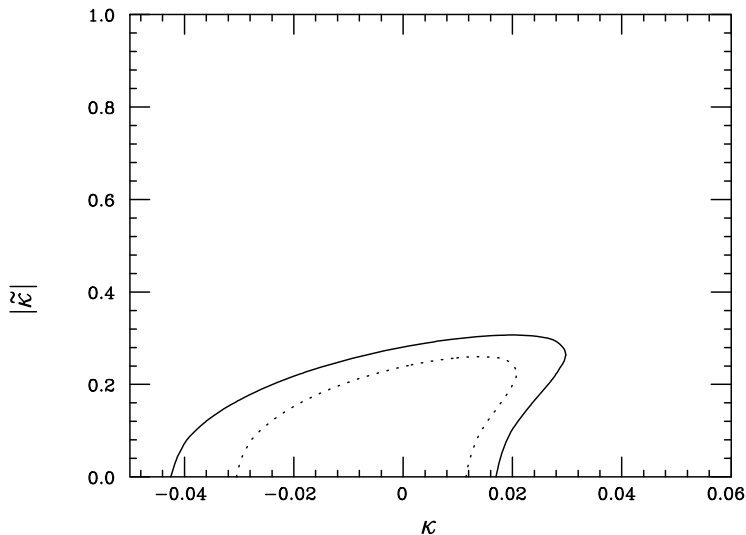


Figure 3: Constraints on anomalous strong moments of the top quark derived from a LC sample of 100  $fb^{-1}$  (solid) and 200  $fb^{-1}$  (dotted) for  $\sqrt{s} = 1$  TeV.

### 3 Two-Photon Physics

At a future  $e^+e^-$  linear collider, the basic interaction process involving two photons,  $e^+e^- \rightarrow e^+e^- + \gamma^{(*)}\gamma^{(*)} \rightarrow e^+e^- + hadrons$ , where the photons involved are various combinations of real ( $\gamma$ ) and virtual ( $\gamma^*$ ) photons, tests QCD in photon structure measurements and in the dynamics of parton distribution function evolution. Direct measurement of the photon structure function  $F_2^\gamma(x, Q^2)$  in  $\gamma\gamma^*$  collisions pushes

into presently unattainable lower  $x$  and higher  $Q^2$  regimes, testing scaling behavior and  $Q^2$  evolution. Extending the measurement of the total  $\gamma\gamma$  cross section to higher  $\sqrt{s}$  tests whether QCD-based models of parton emission describe photon interactions. By colliding two virtual photons, QCD dynamics can be studied in a relatively background-free environment. No other presently planned or anticipated future collider will be able to compete with an  $e^+e^-$  linear collider in these areas.

A comprehensive plan for the study of photon structure through  $e\gamma$  deep inelastic scattering (DIS) and  $\gamma\gamma$  scattering and the study of QCD dynamics through  $\gamma^*\gamma^*$  scattering is presented here. The relative merits of employing photons produced by bremsstrahlung, laser backscattering, and with well-defined polarization are discussed.

### 3.1 Experimental Requirements

Experimental issues related to two-photon physics are mainly concerned with instrumentation of the forward parts of the interaction region (IR), particularly inside the conical shielding masks. In the baseline program for the 500 GeV linear collider, a single IR is envisioned (HEIR), with infrastructure for the inclusion of an additional IR (LEIR) as an upgrade to the baseline. The LEIR would be used for lower energy  $e^+e^-$  interactions and  $\gamma\gamma$  collisions by including a laser system for production of high energy photons. Both IRs require small angle tagging electromagnetic calorimeters in the forward regions used to tag virtual photons from the bremsstrahlung process and, if there is no laser system, hadronic calorimetry from beampipe-to-beampipe for some physics topics.

Virtual photons are produced when, in the bremsstrahlung process, an  $e^+$  or  $e^-$  transfers a significant amount of 4-momentum to the radiated photon. The virtuality,  $Q^2$ , of the “tagged” photon is determined by measuring the energy and angle of the scattered lepton in an electromagnetic calorimeter via the relation

$$Q^2 = 2E_e E'_e (1 - \cos\theta) \quad (2)$$

here  $E_e$  is the incoming lepton beam energy, and  $E'_e$  and  $\theta$  are the scattered lepton energy and angle respectively. Since some physics analyses require that the measurement of  $Q^2$  be as small as possible, the electromagnetic tagging calorimeters must be positioned as closely as possible to the outgoing beampipes on both sides of the interaction region and inside the shielding cone in order to make the minimum measurable scattered lepton angle as small as possible, leading to the requirement of a compact design. Also, since  $Q^2 \simeq E_e E'_e \theta^2$  at small angles, radial position resolution is an important consideration in  $Q^2$  reconstruction, requiring fine-grained readout in the radial direction [16]. Fine-grained sampling calorimeters with these properties have been successfully used in photon-tagging experiments at LEP [17].

In the following subsections, the different methods for producing real and/or almost real photons are discussed.

### 3.1.1 High Energy Interaction Region (HEIR)

In the HEIR, almost real photons ( $Q^2 \simeq 0$ ) are produced solely by the bremsstrahlung process, and are defined by anti-tags in the forward electromagnetic tagging calorimeters. For example, a single tag on one side of the IR, combined with an anti-tag on the other side with hadronic activity in the main detector, signals a  $\gamma^*\gamma$  interaction ( $e\gamma$  DIS). Double anti-tags signal  $\gamma\gamma$  interactions in which both interacting photons are almost real. It is important to note that the energy spectrum of bremsstrahlung-produced photons is dominated by low energy photons. Furthermore, since the untagged photon energy is not known, it is important to have hadronic energy and angle measurement in the forward IR, to as small an angle as possible, in order to determine the kinematics of the interaction.

### 3.1.2 Low Energy Interaction Region (LEIR)

In the LEIR, it is desirable to include a high-power, high repetition-rate laser system which can produce, through the laser backscattering Compton process, high energy real photons [18]. In the Compton scattering process,  $\sim 1$  eV laser photons backscatter from the incoming 250 GeV  $e^+$  or  $e^-$  beam, producing a beam of photons with a high fraction ( $\sim 80\%$ ) of the lepton beam energy and with an energy spread of 5–10%. Since the resulting photon beam spread is small, the kinematics of the high-energy photon interactions can be determined from the known photon energy. Also, since these are high-energy photons at nearly the incoming lepton beam energy,  $W_{\gamma^*\gamma}$  is much larger than that obtained from bremsstrahlung-produced photons, leading to the possibility of reaching very low  $x$  in  $e\gamma$  DIS.

In addition, the polarization state of the interacting photons and/or leptons can have a big effect on the physics impact of a measurement. For example, by combining the transverse polarization of the incoming leptons and the circular polarization of the laser photons in an optimal way, the energy spread of the resulting backscattered photon beam can be reduced by a factor of  $\sim 2$ .

## 3.2 Photon Structure

A real photon can interact both as a point-like particle, or as a collection of quarks and gluons, i.e., like a hadron. The structure of the photon is determined not by the traditional valence quark distributions as in a proton, but by fluctuations of the point-like photon into a collection of partons. As such, the scaling behavior of the photon structure function,  $dF_2^\gamma/d\ln Q^2$ , is always positive. Single tag and double anti-tag events can be used to measure  $F_2^\gamma$  directly and to constrain the relative quark/gluon fractions in the photon, testing predictions for this content and its behavior.

### 3.2.1 $\gamma^*\gamma$ Scattering - $e\gamma$ DIS

Direct measurement of the photon structure function  $F_2^\gamma(x, Q^2)$  in  $e\gamma$  DIS is accomplished by tagging a single virtual photon probe, anti-tagging an almost real or real target photon, and requiring hadronic activity anywhere in the detector.

If the anti-tagged target photon is produced by bremsstrahlung from an incoming lepton, it has very small virtuality,  $\langle Q^2 \rangle \simeq 10^{-4} \text{ GeV}^2$ , and low energy, neither of which is known. In order to determine the longitudinal momentum fraction,  $x$ , the mass  $W_{\gamma^*\gamma}$  of the  $\gamma^*\gamma$  system must be measured, which requires hadronic calorimetry to measure the energy and angle of all hadrons. The best measurements of  $F_2^\gamma$  using bremsstrahlung photons as the target are done at relatively low  $W_{\gamma^*\gamma}$  where it is well-measured away from the forward IR, which in kinematic space is at the high end of the  $x, Q^2$  range. Physics topics which can best be addressed in this region are the scaling behavior of  $F_2^\gamma$  as  $x \rightarrow 1$  and its evolution with  $Q^2$ .

As  $W_{\gamma^*\gamma}$  increases (towards low  $x$ ), increasingly more of the hadronic mass escapes undetected in the beam direction and the actual measurement of the mass, usually referred to as  $W_{vis}$ , begins to differ substantially from the true hadronic mass. Figure 4 illustrates this effect by comparing the measured hadronic mass,  $W_{vis}$  with the true mass,  $W_{\gamma^*\gamma}$ . Monte Carlo simulations of the fragmentation of the  $\gamma^*\gamma$  system are used

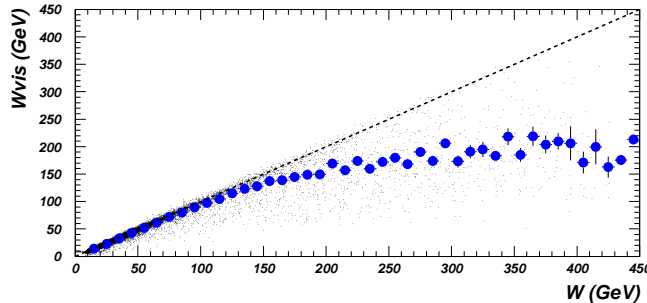


Figure 4: Comparison of  $W_{vis}$  with  $W_{\gamma^*\gamma}$  from PYTHIA [19] for a typical LC detector, including the average value (profile plot).

to correct  $W_{vis}$  for this loss until the uncertainty in the correction begins to dominate the measurement. Eventually, this limits the low  $x$  range of the  $F_2^\gamma$  measurement.

However, if the target photon is produced by laser backscattering, two advantages are realized: 1) the high  $W_{\gamma^*\gamma}$  (low  $x$ ) region is enhanced since the real photon energy is high; and 2) the energy spread of the real photons is small enough such that the error on  $x$  caused by assuming a monochromatic photon is not the dominant source of systematic errors.

Figure 5 shows  $F_2^\gamma$  versus  $Q^2$  for various  $x$  bins from possible measurements at

a future  $e^+e^-$  Linear Collider [20]. The various points are differentiated according to the measurement method. The open squares represent the very low  $x$  region accessible only with photons produced by laser backscattering; open circles represent measurements with target photons from bremsstrahlung and with hadronic calorimetry built into a shielding mask down to  $30\text{ mrad}$ ; solid dots represent measurements with bremsstrahlung photons and with hadronic calorimetry only outside the mask. Note that there is substantial overlap between the methods to provide cross-checks

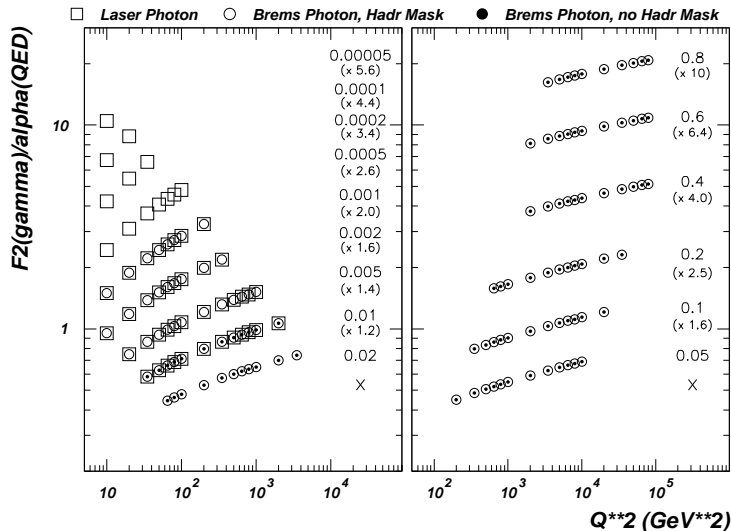


Figure 5:  $F_2^\gamma/\alpha$  versus  $Q^2$  in  $x$  bins. Open squares : real photon target from laser backscattering; open circles : almost-real photon target from bremsstrahlung with small angle hadronic calorimetry; solid dots : almost-real photon target from bremsstrahlung with hadronic calorimetry outside mask.

on the various measurements and experimental conditions.

With known polarization of both the target photon and tagged virtual photon, polarized photon structure functions can be measured for the first time. In addition,  $\ln 1/x$  (BFKL) terms enter in polarized scattering as  $\ln^2 1/x$ , thereby enhancing these effects at low  $x$  over unpolarized scattering. Therefore, in polarized  $e\gamma$  DIS, forward particle and jet measurements, as previously performed at HERA [21], can be done at a future  $e^+e^-$  linear collider with increased sensitivity to any BFKL effects (see section 3.4).

In addition to the  $F_2^\gamma$  structure function,  $e\gamma$  DIS can be used to test QCD in other ways. For example, dijet production in DIS can be used to extract the strong coupling parameter,  $\alpha_s$ , as is done at HERA [22]. At a future  $e^+e^-$  linear collider,  $\alpha_s$  can be compared from  $e^+e^-$  event shapes and from dijets in DIS using the same detector.

### 3.3 $\gamma\gamma$ Scattering – Total Cross Section

Various models have been developed to describe the rise with energy of the total  $\gamma\gamma$  cross section – either a fast rise driven by QCD effects such as minijets, or a slower rise based on reggeon exchange. To get to the highest  $\sqrt{s}$  and  $W_{\gamma\gamma}$ , real photons from the laser backscattering process are required. Studies show that a precision of  $\sim 20\%$  on the total cross section will enable adequate discrimination of model types for energies up to 1 TeV [23]. Figure 6 shows possible  $\sigma_{tot}$  measurements at a 500 GeV linear collider (large stars) compared to existing measurements at lower  $\sqrt{s}$  and to various models.

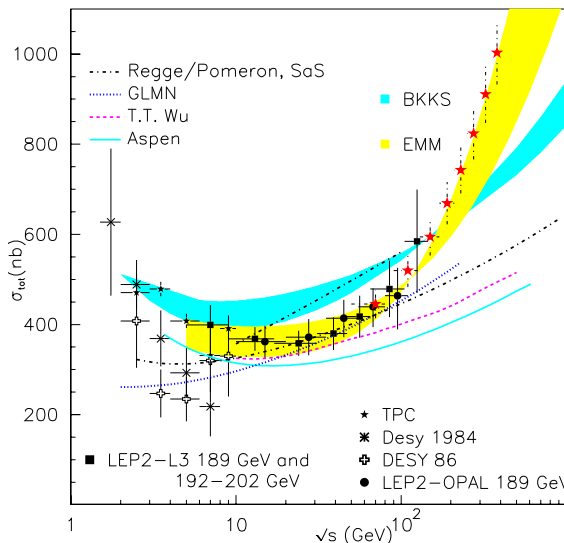


Figure 6:  $\sigma_{tot}$  versus  $\sqrt{s}$  at a LC (large stars) compared to existing data and various models.

Using dijets from  $\gamma\gamma$  scattering, the relative quark/gluon structure of the photon can be determined. Interactions between the almost-real photons produced by bremsstrahlung are determined primarily by interacting gluons in the ratio of approximately 70% gluons and 30% quarks. If real photons from laser backscattering are used, an almost pure gluon constituted photon can be investigated (90% $g$ /10% $q$ ) [24].

### 3.4 $\gamma^*\gamma^*$ Scattering - QCD Dynamics

Double tagged virtual photon scattering completes the study of the photon at the linear collider by allowing the evolution of photon structure to be studied in an almost background-free environment. The  $Q^2$  of each the scattered leptons (denoted  $Q_1^2$  and  $Q_2^2$ ) is measured in the forward electromagnetic tagging calorimeters. By requiring the ratio  $Q_1^2/Q_2^2 \sim 1$ , production of hadrons in the region between the two virtual

photons through traditional DGLAP evolution is suppressed. This suppression grows stronger as the rapidity separation,  $Y$ , between the two virtual photons increases. At large values of  $Y$ , any signal above the small DGLAP background points to alternative forms of structure function evolution, e.g. to the  $\ln(1/x)$  evolution of BFKL. Virtual photon scattering at a linear collider provides perhaps the cleanest environment in which to study BFKL physics [25,26].

With total center-of-mass energy  $s$  and photon virtuality  $-Q^2$ , BFKL effects are expected in the kinematic region where the square of the photon-photon invariant mass (or, equivalently, the hadronic final-state system) is large, and

$$s \gg Q^2 \gg \Lambda_{QCD}^2.$$

At fixed order in QCD, the dominant process is four-quark production with  $t$ -channel gluon exchange (each photon couples to a quark box; the quark boxes are connected via the gluon). The corresponding BFKL contribution arises from diagrams with a gluon ladder attached to the  $t$ -channel gluon. At lepton-hadron or hadron-hadron colliders, the presence of hadrons in the initial state can complicate or even mask BFKL effects.

The largest values of  $Y$  are obtained at low  $Q_{1,2}^2$ , again emphasizing the need for the electromagnetic tagging calorimeters to be positioned as close to the beampipe as possible. Figure 7 shows the substantially greater reach in  $Y$  available to the 500 GeV LC relative to that of LEP2 running at 189 GeV.

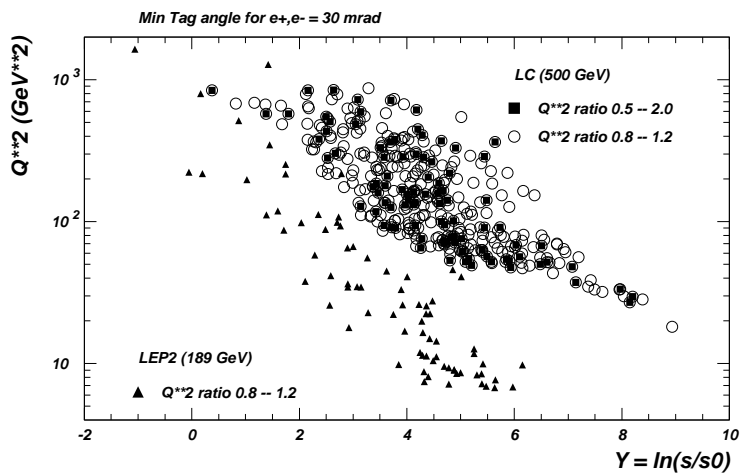


Figure 7:  $Q^2$  versus  $Y$  for a 500 GeV LC compared to LEP2.

Experiments at LEP have looked for BFKL effects in virtual photon scattering [27]. The data tend to lie between the predictions of fixed-order QCD and analytic solutions to the BFKL equation (asymptotic full-order QCD). However, the data were

compared to the asymptotic QCD prediction in a non-asymptotic regime [28], so the disagreement with QCD is not surprising. In contrast, a linear collider will be expected to better reach the asymptotic regime, providing a more definitive test of BFKL. Improved predictions are also on the way with the development of BFKL Monte Carlo programs that incorporate kinematic constraints, such as [29]. On the more theoretical front, next-to-leading log corrections have been calculated and found to be large, but the source of the large corrections is understood and they are being brought under control; see [30] for a review and references.

### 3.5 Summary of Two-photon Physics

Two-photon physics from  $e^+e^-$  collisions has grown tremendously in the past several years of higher energy LEP2 running and will continue to provide a wealth of precision measurements at a future  $e^+e^-$  linear collider. Using combinations of tagged and untagged bremsstrahlung photons, aspects of real and virtual photon structure will be addressed, especially  $F_2^\gamma$  at high  $Q^2$ , the relative quark/gluon content of the photon from dijets, and possible BFKL effects in the QCD evolution.

With laser-backscattered real photons, the highest energies available at the linear collider can be fully exploited.  $F_2^\gamma$  can be measured at very low  $x$ , which in combination with high  $Q^2$  measurements from bremsstrahlung photons, will map out a kinematic region in photon structure as extensive as that known for the proton. The total  $\gamma\gamma$  cross section will also be measured at the highest  $\sqrt{s}$  available at the linear collider, leading to understanding of the dominant mechanisms responsible for this interaction.

Finally, with combinations of lepton and photon polarization, BFKL effects can be enhanced and the first measurements of polarized structure functions of the photon can be made.

## 4 Overall Summary and Conclusions

The High Energy Linear Collider offers a unique program of QCD and related two-photon studies. The strong coupling constant  $\alpha_S$  can be measured at high  $Q^2$  to a precision approaching  $\pm 1\%$ , free of the initial-state ambiguities which make the corresponding determination at a hadron collider substantially less precise, and allowing for substantial improvements in the determination of the running of the QCD coupling strength, as well as its extrapolation to the GUT scale. Constraints on the strong coupling properties of the top, providing sensitivity to a number of new physics scenarios inspired by the large mass of the top quark, can be made as much as an order of magnitude more stringent at an  $e^+e^-$  collider than at a proton collider of equivalent reach.

On the two-photon front, the precisely defined state of the incoming electron and positron beams permits the kinematic properties of the interacting virtual and nearly on-shell photons to be inferred from the properties of the recoiling electrons. This in turn allows for a unique program of photon structure and strong-force dynamics which can not be emulated by any other proposed facility. In addition, the possibility of precisely controlled real photons beams from the Compton backscattering of polarized laser light opens up further vistas in the exploration of photon structure, and may allow the resolution of long-standing questions regarding the energy evolution of the photon-photon total cross section. Again, these studies are only possible within the larger context of an  $e^+e^-$  Linear Collider program.

Together, these physics topics present a unique and compelling program of strong-interaction studies at a High Energy Linear Collider, and one which adds substantial weight to the promise of the proposed Linear Collider physics program.

## References

- [1] See *eg.* S. Bethke, J. Phys. **G26**: R27 (2000).
- [2] See *eg.* P.N. Burrows, Proc. XXVIII International Conference on High Energy Physics, Warsaw, Poland, July 25-31 1996, Eds. Z. Adjuk, A.K. Wroblewski, World Scientific 1997, p. 797.
- [3] S. Bethke, Proc. Workshop on Physics and Experiments with Linear  $e^+e^-$  Colliders, 26-30 April 1993, Waikoloa, Hawaii; World Scientific, Eds. F.A. Harris *et al.*, Vol. II p. 687.
- [4] B. Schumm, SCIPP-96-45, hep-ex/9612013 (1996).
- [5] B. A. Schumm and A. S. Truitt, To appear in the proceedings of 5th International Linear Collider Workshop (LCWS 2000), Fermilab, Batavia, Illinois, 24-28 Oct 2000; e-Print Archive: hep-ex/0102020
- [6] O. Biebel, PITHA 99/40, MPI-PhE/99-17, LC-PHSM-2000-003, hep-ex/9912051, Phys.Rept. 340:165, 2001.
- [7] See, for example, OPAL Collaboration, OPAL Physics Note PN377.
- [8] S. Catani *et al.*, Nucl. Phys. **B407** 3 (1993).
- [9] Z. Bern, L. Dixon, and D.A. Kosower, JHEP 0001:027,2000
- [10] See *eg.* M. Neubert, Nucl. Phys. **B463** (1996) 511; G. Altarelli, P. Nason, G. Ridolfi, Z. Phys. **C68** (1995) 257.
- [11] RG trajectories calculated in Paul Langacker and Nir Polonsky, Phys. Rev. D52:3081-3086, 1995.
- [12] T. G. Rizzo, hep-ph/9605361, May 1996.
- [13] D. Atwood, A. Kagan, and T.G. Rizzo, Phys. Rev. D52:6264-6270, 1995

- [14] T. G. Rizzo, hep-ph/9506351, August 1995.
- [15] L.N. Lipatov, Sov. J. Nucl. Phys. **23** (1976) 338; E.A. Kuraev, L.N. Lipatov and V.S. Fadin, Sov. Phys. JETP **45** (1977) 199; Ya.Ya. Balitsky and L.N. Lipatov, Sov. J. Nucl. Phys. **28** (1978) 822.
- [16] S.R. Magill, proc. Worldwide Study on Physics and Experiments with Future Linear  $e^+e^-$  Colliders, Sitges, Barcelona, Spain, April28-May5, 1999, 1066.
- [17] R. Barate et al. (ALEPH), Phys. Lett. B458 (1999) 152. M. Acciarri et al. (L3), Phys. Lett. B436 (1998) 403. K. Ackerstaff et al. (OPAL), Phys. Lett. B412 (1997) 225-234. P. Abreu et al. (DELPHI), Zeit. Phys. C69 (1996) 223.
- [18] V.G. Serbo, proc. International Workshop on High Energy Photon Colliders, DESY Hamburg, Germany, June 14-17, 2000, to be published in Nucl. Inst. Meth. A., and references therein.
- [19] T. Sjöstrand, Comp. Phys. Comm. 82 (1994) 74.
- [20] S.R. Magill, talk given at 2nd International Workshop on High Energy Photon Colliders, Fermilab, USA, March 14-17, 2001.
- [21] J. Breitweg et al. (ZEUS), Eur. Phys. Jour. C6 (1998) 41-56; C. Adloff et al. (H1), Phys. Lett. B462 (1999) 440-452.
- [22] J. Breitweg et al. (ZEUS), DESY 01-018 (February 2001), accepted by Phys. Lett. B; C. Adloff et al. (H1), DESY 00-181 (December 2000), submitted to Eur. Phys. J. C.
- [23] R.M. Godbole and G. Pancheri, proc. International Linear Collider Workshop (LCWS2000), Fermilab, USA, October 26-30, 2000.
- [24] T. Wengler and A. De Roeck, proc. International Workshop on High Energy Photon Colliders, DESY Hamburg, Germany, June 14-17, 2000, to be published in Nucl. Inst. Meth. A.
- [25] S.J. Brodsky, F. Hautmann and D.E. Soper, Phys. Rev. **D56**, 6957 (1997).
- [26] M. Boonekamp, A. De Roeck, C. Royon and S. Wallon, Nucl. Phys. B **555**, 540 (1999) [hep-ph/9812523].
- [27] See, e.g., A. De Roeck, Nucl. Phys. Proc. Suppl. **99**, 144 (2001) and references therein.
- [28] L. H. Orr and W. J. Stirling, proc. 30th International Conference on High-Energy Physics (ICHEP 2000), Osaka, Japan, 27 Jul - 2 Aug 2000, hep-ph/0012198.
- [29] C.R. Schmidt, Phys. Rev. Lett. **78** (1997) 4531; L.H. Orr and W.J. Stirling, Phys. Rev. **D56** (1997) 5875.
- [30] G. P. Salam, Acta Phys. Polon. **B30**, 3679 (1999); proc. 35th Rencontres de Moriond: QCD and High Energy Hadronic Interactions, Les Arcs, Savoie, France, 18-25 March 2000, hep-ph/0005304, and references therein.